MULTISPECTRAL IMAGE FUSION USING SLANTLET-BASED RIDGELET TRANSFORM

TARIQ ZEYAD ISMAEEL   **AHMED FREIDOON FADHIL**
Electrical Engineering   **Electrical Engineering**
Baghdad University   **Baghdad University**

ABSTRACT

   This paper introduces a new method in the multispectral image fusion based on ridgelet transform which represents edges better than wavelets. Since edges play a fundamental rule in image understanding, one good way to enhance spatial resolution is to enhance the edges. Ridgelet based image fusion method provides richer information in the spatial and spectral domains simultaneously. Also another method introduced based on new Hybrid transform which is improvement from the Ridgelet transform. Here we used our method to merge the panchromatic image of IKONOS sensor (1m resolution) with its multispectral image (4m resolution). The software used in this paper is (Matlab V 7.0.4).

الخلاصة

هذا المشروع يقدم طريقة جديدة في دمج الصور بالاعتماد على التحويل (Ridgelet) التي تقوم باسترجاع الحافات في الصور بطريقة أفضل من التحويل (Wavelet). ولان الحافات تلعب دوراً رئيسياً في فهم معالم الصور، فان احدى الطرق الجيدة لزيادة الوضوحية هو استرجاع معلومات أفضل عن الحافات. إن طريقة دمج الصور المعتمدة على التحويل (Ridgelet) يقوم باعطاء معلومات أغنى في المجالين في استرجاع الأطياف اللونية وكذلك في زيادة الوضوحية للصور . ايضاً طريقة أخرى قدمت والتي تستند على تحويل مركب والذي هو تحسين للتحويل (Ridgelet). هنا استخدمنا في طريقتنا لدمج صور ذات وضوحية عالية مأخوذة من القمر (IKONOS) وضوحيتها (1m) مع صور متعددة الأطياف وضوحيتها (4m) . البرنامج المستخدم في هذا المشروع هو (Matlab V 7.0.4) .

KEY WORDS
Image fusion, wavelet transform, ridgelet transform, correlation, spectral, spatial, fusion rule.

INTRODUCTION

   There are different cases that high spectral and spatial resolution are needed both together, but the instruments presented now can't produce such data because of several limitations, One solution to get such data is data fusion (Dehghani M. 2003).

   Image fusion, in general, can be described as a process of producing a single image from two or more images that are collected from the same or different sensors. The objective of the fusion process is to keep maximum spectral information from the original multispectral image while increasing the spatial resolution. Military, medical imaging, computer vision, robotic industry and remote sensing are some of the fields benefiting from the image fusion (Gungor O. 2003).

STANDARD FUSION METHODS

In remote sensing and in geomatics, the methods most often used for fusing images with different resolutions are:

IHS Method:

This method is based on the transformation of RGB (Read- Green- Blue) multispectral channels into IHS (Intensity- Hue-Saturation). A simple model for the IHS transformation is given in (Genderen V. 1998). this model is implemented in much commercial software. The conversion equations are:

$$
\begin{bmatrix} I \\ V_1 \\ V_2 \end{bmatrix} = \begin{bmatrix} 1/3 & 1/3 & 1/3 \\ 1/\sqrt{6} & 1/\sqrt{6} & -2/\sqrt{6} \\ 1/\sqrt{2} & -1/\sqrt{2} & 0 \end{bmatrix} \begin{bmatrix} R \\ G \\ B \end{bmatrix}
\tag{1}
$$

$$
H = \tan^{-1}\left(\frac{V_2}{V_1}\right)
\tag{2}
$$

$$
S = \sqrt{V_1^2 + V_2^2}
\tag{3}
$$

Where V_1, and V_2 are intermediate variables. The inverse IHS transformation is computed as follows:

$$
\begin{bmatrix} R \\ G \\ B \end{bmatrix} = \begin{bmatrix} 1 & 1/\sqrt{6} & 1/\sqrt{2} \\ 1 & 1/\sqrt{6} & -1/\sqrt{2} \\ 1 & -2/\sqrt{6} & 0 \end{bmatrix} \begin{bmatrix} P* \\ V_1 \\ V_2 \end{bmatrix}
\tag{4}
$$

Where P* is the Panchromatic image stretched to I.

- Brovey Method:

In this method, the MS image is normalized and each band of the fused MS image is obtained by multiplying the normalized MS bands with the panchromatic image. The Brovey transform can be expressed as (Vijayaraj V. 2004):

$$
R_{new} = \frac{R}{R+G+B} * PAN
\tag{5}
$$

$$
G_{new} = \frac{G}{R+G+B} * PAN
\tag{6}
$$

$$
B_{new} = \frac{B}{R+G+B} * PAN
\tag{7}
$$

Where PAN is the Panchromatic Image, MS is the Multispectral Image, (R, G, B)$_{new}$ are the new bands of (Red, Green, Blue).

- Wavelet Decomposition Method:

The 2-D (2-D is Two-Dimensional) Discrete Wavelet Transform (DWT) is used for image fusion process. Wavelet transform is defined as the sum over all time of the signal multiplied by scaled, shifted version of the mother wavelet. Similar to the Fourier analysis that breaks a signal into different sine waves of different frequencies, wavelet transform decomposes a signal into the scaled and/or shifted versions of the mother wavelet (Gungor O. 2003).

In DWT, instead of calculating wavelet coefficients at every possible scale, the scales and shifts are usually based on power of two if we have a mother wavelet.

The DWT of a signal x is calculated by passing it through a series of filters. First the samples are passed through a low pass filter with impulse response g resulting in a convolution of the two, see eq. (8):

$$y[n] = (x * g)[n] = \sum_{k=-\infty}^{\infty} x[k] \cdot g[n - k] \qquad (8)$$

The signal is also decomposed simultaneously using a high-pass filter h. The output gives the detail coefficients (from the high-pass filter) and approximation coefficients (from the low-pass filter). It is important that the two filters are related to each other and they are known as a quadrature mirror filter. However, since half the frequencies of the signal have now been removed, half the samples can be discarding according to Nyquist's rule.

For many signals, the low-frequency content is the most important part. It is what gives the signal its identity. The high-frequency content, on the other hand, imparts flavor or nuance. Consider the human voice. If you remove the high-frequency components, the voice sounds different, but you can still tell what's being said. However, if you remove enough of the low-frequency components, you hear gibberish. In wavelet analysis, all the speaking is about the approximations and details. The approximations are the high-scale, low-frequency components of the signal. The details are the low-scale, high-frequency components (Saleh Z. J. 2004).

The filter outputs are then down sampled by 2, as shown in eq. (9) and eq. (10):

$$y_{\text{low}}[n] = \sum_{k=-\infty}^{\infty} x[k] \cdot g[2 \cdot n - k] \qquad (9)$$

$$y_{\text{high}}[n] = \sum_{k=-\infty}^{\infty} x[k] \cdot h[2 \cdot n - k] \qquad (10)$$

This decomposition has halved the time resolution since only half of each filter output characterizes the signal. However, each output has half the frequency band of the input so the frequency resolution has been doubled. As shown in **Fig. 1.**
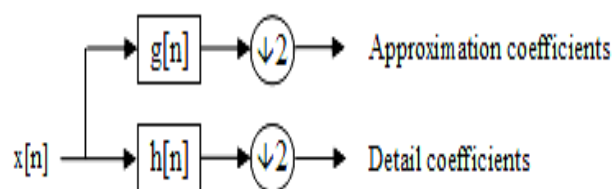

Fig. (1)
Block diagram of filter analysis

This decomposition is repeated to further increase the frequency resolution and the approximation coefficients decomposed with high and low pass filters and then down-sampled. This is represented as a binary tree with nodes representing a sub-space with different time-frequency localization. The tree is known as a bank. As shown in **Fig. 2.**
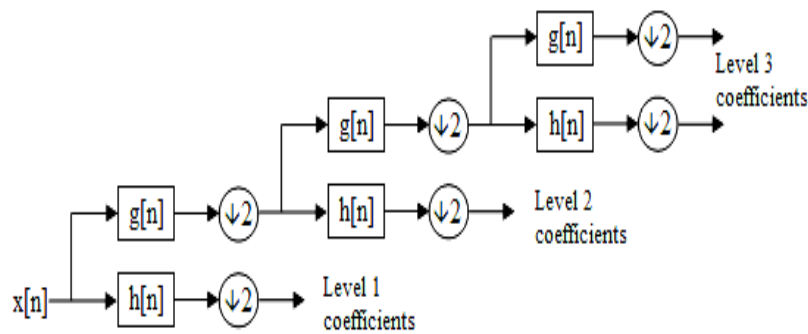
Fig. (2)
A 3 level filter bank (A 3 level DWT).

At each level in the above diagram the signal is decomposed into low and high frequencies. Due to the decomposition process the input signal must be a multiple of (2^n) (where n is the number of levels).

The image decomposition is usually a lossless process which converts the image data from the spatial domain to frequency domain, where the transformed coefficients are decorrelated. First level of image (2-D Signal) decomposition partitions image data into four sub-bands labeled as LL_1, HL_1, LH_1, and HH_1, as shown in **Fig. 3(a).** Each coefficient represents a spatial area corresponding to one-quarter of the original image size. The low frequencies represent a bandwidth corresponding to $0 < |\omega| < \pi/2$, while the high frequencies represent the band $\pi/2 < |\omega| < \pi$. To obtain the next level of decomposition, the LL_1 sub-band is further decomposed into the next level of four sub-bands, as shown in **Fig. 3(b)**. The low frequencies of the second level decomposition correspond to $0 < |\omega| < \pi/4$, while the high frequencies at the second level decomposition correspond to $\pi/4 < |\omega| < \pi/2$. This decomposition can be continued to as many levels as needed (Saleh Z. J. 2004).

Where H is the High Subband, HH is the High High Subband, HL is the High Low Subband, L is the Low Subband, LH is the Low High Subband, and LL is the Low Low Subband
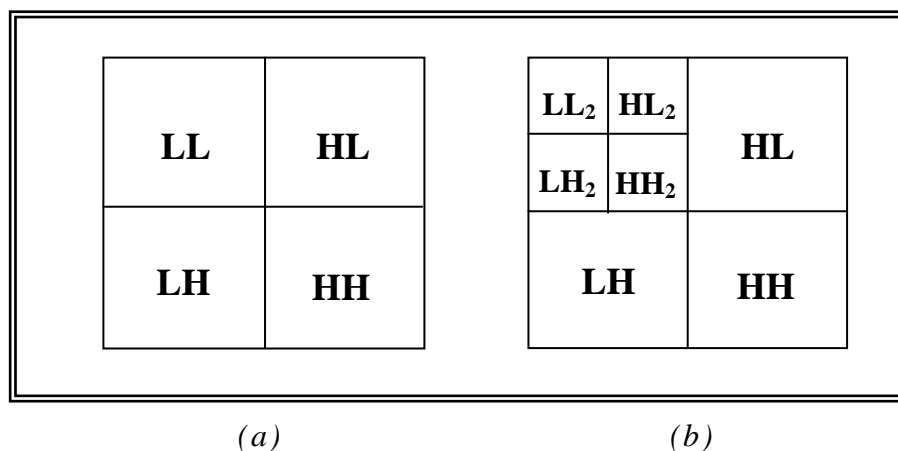

(a)   *(b)*

Fig. (3): 2-D Wavelet Transform. (a) First-level Decomposition.
(b) Second –level Decomposition. (L denotes a low band, H denotes a high band, and the subscript denotes the number of the level).

For a length-2 h(n), there are no degrees of freedom left after satisfying the required conditions. These requirements are (Burrus C. S. 1998):

$$\left.\begin{array}{l} h\left(0\right)+h\left(1\right)=\sqrt{2} \\ h^{2}\left(0\right)+h^{2}\left(1\right)=1 \end{array}\right\} \tag{11}$$

Which are uniquely satisfied be:

$$h_{D2}=\{h(0),h(1)\}=\left\{\frac{1}{\sqrt{2}},\frac{1}{\sqrt{2}}\right\}$$

(12)

These are the Haar scaling function coefficients, which are also the length-2 Daubechies coefficients.

For the length-4 coefficients sequence, there is one degree of freedom or one parameter that gives all the coefficients that satisfy the required conditions (Burrus C. S. 1998):

$$\left.\begin{array}{l} h\left(0\right)+h\left(1\right)+h\left(2\right)+h\left(3\right)=\sqrt{2} \\ h^{2}\left(0\right)+h^{2}\left(1\right)+h^{2}\left(2\right)+h^{2}\left(3\right)=1 \\ h\left(0\right)h\left(2\right)+h\left(1\right)h\left(3\right)=0 \end{array}\right\} \tag{13}$$

Letting the parameter be the angle α, the coefficients become

$$\left.\begin{array}{l} h(0)=(1-\cos\alpha+\sin\alpha)/(2\sqrt{2}) \\ h(1)=(1+\cos\alpha+\sin\alpha)/(2\sqrt{2}) \\ h(2)=(1+\cos\alpha-\sin\alpha)/(2\sqrt{2}) \\ h(3)=(1-\cos\alpha-\sin\alpha)/(2\sqrt{2}) \end{array}\right\} \tag{14}$$

These equations (14) give length-2 Haar coefficients for α=0, π/2, 3π/2 and length-4 Daubechies coefficients for α=π/3. These Daubechies-4 coefficients have a particularly clean form:

$$h_{D4}=\left\{\frac{1+\sqrt{3}}{4\sqrt{2}},\frac{3+\sqrt{3}}{4\sqrt{2}},\frac{3-\sqrt{3}}{4\sqrt{2}},\frac{1-\sqrt{3}}{4\sqrt{2}}\right\}$$

(15)

The algorithm of image fusion using DWT described in the following steps:

. Size of inputs images:

Given a two dimensional images (example, image A, image B) it is necessary to convert it into the same size a power of two square forms. This is necessary in order to facilitate the application of the FDWT transform. If the image is not a square matrix, then, a resize operation should be performed to the image.

. Conversion of multispectral (RGB) image to IHS space:

In this step the MS image will be converted from the RGB model to the IHS model.

. Computation of two dimensions FDWT:

In this step, the two dimensional Fast Discrete Wavelet Transform (FDWT) should be applied to the resized two dimensional images. This paper will take Second-Level decomposition for the Wavelet Transform.

. Fusion rule:

The most used image fusion rule based on wavelet transform is maximum selection, compare the two coefficients of FDWT of the two images and select the maximum between them. But this rule leads to a color distortion. Another rule which proposed by (Garzelli A. 2004). The different rule applied to the high frequency and low frequency bands, all the high frequency bands (LH, HL, HH) contain transform values that fluctuate around zero (Saleh Z. J. 2004). While the lowpass subband is an approximation of the input image. The three detail subbands convey information about the detail parts in horizontal, vertical and diagonal directions. Different merging procedures will be applied to approximation and detail subbands. Lowpass subband will be merged using simple averaging operations since they both contain approximations of the source images. A selection procedure will be applied to the wavelet coefficients of the three detail subbands. The selection rule used for the detail subbands are maximum selection rule (for complex values it selects maximum real value).

. Invere fast discrete wavelet transforms:

After selected the fused low frequency and high frequency bands, fused coefficient is reconstructed using the Inverse fast discrete wavelet transform to get the fused image which represent the new I band.

. Inverse (IHS) to (RGB) image:

The resultant image which represents the new I band will be back transformed with the original H & S bands to the RGB model. Then these three bands represent the new MS image.

HYBRID TRANSFORMS

- Discrete Ridgelet Transform

The main idea behind the Ridglet transform is first to apply the two dimensions Discrete Fourier Transform (2-D DFT) to the two dimensions signal (image). Next, to map line sampling scheme into a point sampling scheme using the Radon transform. Hence, it is required to take the one

dimension inverse Discrete Fourier Transform (1-D IDFT) for each column of the produced two dimensions signal. Finally, it is required to perform the Wavelet transform to each row of the resultant two dimensions signal. Thus the structure of this transform consists of four fundamentals parts, these are (Granai L., 2003):

  a) Two dimensions Discrete Fourier Transform (2-D DFT).

  b) Radon Transform (RT).

  c) One dimension inverse Discrete Fourier Transform (1-D IDFT).

  d) One dimension Discrete Wavelet Transform (1-D DWT)

   It is expected that this transform will give a high performance and strong properties. This is because combines together the good properties of the local transforms.

- Improved Ridgelet Transform

   The main idea of this improvement is to replace the wavelet transform in the Ridgelet transform structure by the slantlet transform. Since the slantlet transform is an orthogonal DWT and provides improved time localization than the DWT (Panda G. 2002). So that this new hybrid transform will give a high performance and strong properties.

THE SLANTLET TRANSFORM

   The Slantlet uses a special case of a class of bases described by (Alpert B. 1993), the construction of which relies on Gram–Schmidt orthogonalization. The Slantlet is based on a filterbank structure where different filters are used for each scale. Let us consider a usual two-scale iterated DWT filterbank shown in **Fig. 4(a)** and its equivalent form **Fig. 4(b).** The Slantlet filterbank employs the structure of the equivalent form shown in **Fig. 4(b)** but it is occupied by different filters that are not products. With this extra degree of freedom obtained by giving up the product form, filters of shorter length are designed satisfying orthogonality and zero moment conditions (Panda G. 2002).

   For two-channel case the Daubechies filter (Daubechies I. 1992) is the shortest filter which makes the filterbank orthogonal and has K zero moments. For K=2 zero moments the iterated filters of **Fig. 4(b)** are of lengths 10 and 4 but the Slantlet filterbank with K=2 zero moments shown in **Fig. 5** has filter lengths 8 and 4. Thus the two-scale Slantlet filterbank has a filter length which is two samples less than that of a two-scale iterated Daubechies-2 filterbank. This difference grows with the number of stages. Some characteristic features of the Slantlet filterbank are orthogonal, having two zero moments and has octave-band characteristic. Each filterbank has a scale dilation factor of two and provides a multiresolution decomposition. The slantlet filters are piecewise linear.

Even though there is no tree structure for Slantlet it can be efficiently implemented like an iterated DWT filterbank (Selesnick I. W. 1999). Therefore, computational complexities of the Slantlet are of the same order as that of the DWT. The filter coefficients used in the Slantlet filterbank as derived in (Selesnick I. W. 1999) are given by:

$$E_0(z) = (-\frac{\sqrt{10}}{20} - \frac{\sqrt{2}}{4}) + (\frac{3\sqrt{10}}{20} + \frac{\sqrt{2}}{4})z^{-1}$$
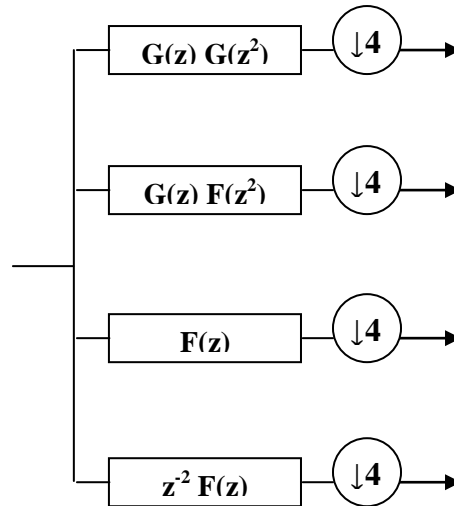$$+ (-\frac{3\sqrt{10}}{20} + \frac{\sqrt{2}}{4})z^{-2} + (\frac{\sqrt{10}}{20} - \frac{\sqrt{2}}{4})z^{-3}$$

(16)

$$E_1(z) = (\frac{7\sqrt{5}}{80} - \frac{3\sqrt{55}}{80}) + (-\frac{\sqrt{5}}{80} - \frac{\sqrt{55}}{80})z^{-1}$$
$$+ (-\frac{9\sqrt{5}}{80} + \frac{\sqrt{55}}{80})z^{-2} + (-\frac{17\sqrt{5}}{80} + \frac{3\sqrt{55}}{80})z^{-3}$$
$$+ (\frac{17\sqrt{5}}{80} + \frac{3\sqrt{55}}{80})z^{-4} + (\frac{9\sqrt{5}}{80} + \frac{\sqrt{55}}{80})z^{-5}$$
$$+ (\frac{\sqrt{5}}{80} - \frac{\sqrt{55}}{80})z^{-6} + (-\frac{7\sqrt{5}}{80} - \frac{3\sqrt{55}}{80})z^{-7}$$

(17)

$$E_2(z) = (\frac{1}{16} + \frac{\sqrt{11}}{16}) + (\frac{3}{16} + \frac{\sqrt{11}}{16})z^{-1}$$
$$+ (\frac{5}{16} + \frac{\sqrt{11}}{16})z^{-2} + (\frac{7}{16} + \frac{\sqrt{11}}{16})z^{-3}$$
$$+ (\frac{7}{16} - \frac{\sqrt{11}}{16})z^{-4} + (\frac{5}{16} - \frac{\sqrt{11}}{16})z^{-5}$$
$$+ (\frac{3}{16} - \frac{\sqrt{11}}{16})z^{-6} + (\frac{1}{16} - \frac{\sqrt{11}}{16})z^{-7}$$

(18)

(19)

$$E_3(z) = z^{-3} E_2(\frac{1}{z})$$
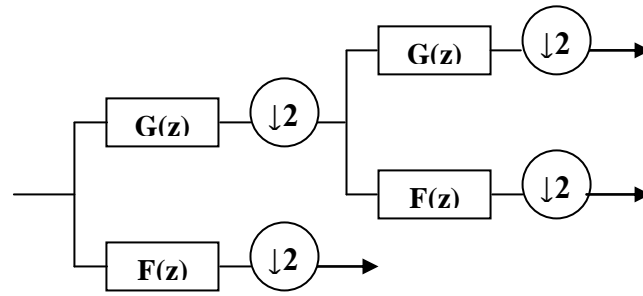
(a)

(b)

Fig. (4): Two-scale iterated filterbank and its equivalent form using the DWT.
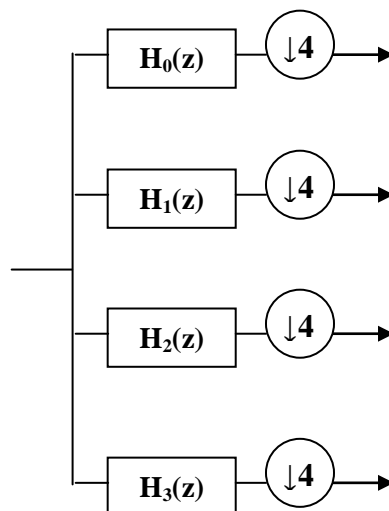

Fig. (5): Two-scale filterbank structure using the Slantlet

IMAGE FUSION RESULTS FOR IKONOS IMAGES

The IKONOS Panchromatic (1 meter spatial resolution) and multispectral image (4 meter spatial resolution) of a sub-urban area are shown in **Fig. 6(a)** and **Fig. 6(b)** respectively. Different fusion methods applied to this data set to produce the fused multispectral images in **Fig. 6(c), (d), (e), (f), (g), (h), (i),** and **(j) .** The Corr were computed as shown in **Table 1,** and **Table 2.** The Corr values are computed between bands of the new fused image each one with its original multispectral one, also computed between each with the original panchromatic one.
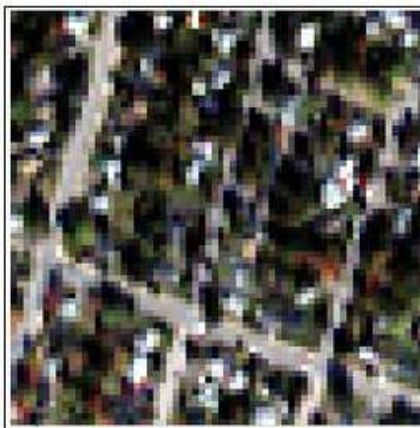
(a)   *(b)*   *(c)*

(g)   *(h)*   *(i)*

IMAGE FUSION USING HYBRID TRANSFORM

The steps of image fusion Using Hubrid Transforms are the same of the steps of image fusion using the Wavelet Transform, The difference is replacing the FDWT by the Hybrid Transform.

Fig. 6: (a) PAN image (b) MS image ($\times$ 4 zoom) (c) Fused IHS image (d) Fused Brovey image (e) Fused DWT based (haar) image (f) Fused DWT based (Db4) image (g) Fused DRGT based (haar) image (h) Fused DRGT based (Db4) image (i) Fused IRGT image.

Table 1: The Corr values between each new image band with its original MS band computed for the different fusion methods.

Method	R & new R ideal value (1)	G & new G ideal value (1)	B & new B ideal value (1)
IHS method	0.4781	0.4630	0.4134
Brovey method	0.4160	0.4336	0.5004
DWT based (haar)	0.7664	0.7595	0.7498
DWT based (Db4)	0.7864	0.7800	0.7718
DRGT based (haar)	0.8116	0.8060	0.8007
DRGT based (Db4)	0.8190	0.8136	0.8085
IRGT	<u>0.8456</u>	<u>0.8410</u>	<u>0.8390</u>

Where Corr is the Correlation Coefficient, Db4 is Duabchies 4-Tap Wavelets, DRGT is Discrete Ridgelet Transform, and IRGT is Improved Ridgelet Transform. The ideal values in **Table 1** represents the Corr values between each original MS band with its self.

Table 2: The Corr values between each new image band with the original panchromatic image computed for the different fusion methods.

Method	PAN & new R ideal value (0.4702)	PAN & new G ideal value (0.4673)	PAN & new B ideal value (0.3719)
IHS method	0.9911	0.9945	0.9863
Brovey method	0.9319	0.9429	0.8854

DWT based (haar)	0.8315	0.8326	0.7757
DWT based (Db4)	0.8281	0.8293	0.7720
DRGT based (haar)	0.8408	0.8425	0.7849
DRGT based (Db4)	0.8382	0.8399	0.7824
IRGT	0.8623	0.8649	0.8082

The Ideal value in **Table 2** represents the Corr values between each original MS image band with the original panchromatic image.

SUBJECTIVE AND OBJECTIVE EVALUATIONS

Subjective Evaluation

The objective of fusion is to increase the spatial resolution of MS image while retaining the multispectral information from MS image. Therefore, subjective analysis is a necessity to check if the objective of fusion has been met.

For Subjective evaluation, two approaches are used. First, the proposed fusion algorithm is evaluated in terms of spatial and spectral improvements. It is clearly seen from the fused images in **Fig. 6** that the spatial resolutions of the images after the fusion are improved and the fused image appears brighter than the original one and the vegetated areas appear coarser. In the original MS images, it is very difficult to discern some physical features like small buildings, and small roads that can be apparently seen in the fused images. The fused images also keep the original colors that means that the spectral content of the images are carried to the fused ones. Therefore, the fused images will significantly improve the image classification results.

Secondly, as a comparison, the same images are fused also using IHS, Brovey, and DWT image fusion techniques. It is seen that these fusion methods also improve the spatial resolution. But, the colors of the features in the fused images are changed. This color distortion effect is the largest in Brovey method. Among these three methods, DWT method gives the best result in terms of color conservation.

Objective Evaluation

In general, a good fusion approach should retain the maximum spatial and spectral information from the original images and should not damage the internal relationship among the original bands. Based on these three criteria, Correlation Coefficients are used to objectively evaluate the image fusion results.

The closeness between two images can be quantified in terms of the correlation function. The correlation coefficient ranges from –1 to +1. A correlation coefficient value of +1 indicates that the two images are highly correlated, i.e., very close to one another. A correlation coefficient of –1 indicates that the two images are exactly opposite to each other (Eskicioglu A. 1995). The correlation coefficient is computed from:

$$Corr\ (I,F) = \frac{\sum\limits_{r=1}^{N}\sum\limits_{c=1}^{N}\left(I(r,c)-\bar{I}\right)\left(F(r,c)-\bar{F}\right)}{\sqrt{\left(\sum\limits_{r=1}^{N}\sum\limits_{c=1}^{N}\left(I(r,c)-\bar{I}\right)^2\right)\left(\sum\limits_{r=1}^{N}\sum\limits_{c=1}^{N}\left(F(r,c)-\bar{F}\right)^2\right)}} \tag{22}$$

Where I is the ideal image, F is the fused image, $\bar{I}$ and $\bar{F}$ stand for the mean values of the corresponding data set, and N×N is the image size.

Here I and F are the two images between which the correlation is computed. Correlation coefficients between two different sets of image bands were computed. The correlation between each band of the multispectral image before and after sharpening was computed. The best spectral information is available in the multispectral image and hence the pansharpened image bands should have a correlation closer to that between the multispectral image bands. The spectral quality of the sharpened image is good if the correlation values are closer to each other. Another set of correlation coefficients was computed between each band of the multispectral image and the panchromatic image. Since the panchromatic image has better spatial information, the correlation between the sharpened image bands and the pan image is expected to increase compared to that of the original multispectral. An increase in the correlation indicates an increase in the spatial information compared to the multispectral image.

Table 1 lists the Corr values between the original MS bands and their corresponding original image bands. The higher the value, the more similar the fused image to the corresponding original image, which in turn indicates good spectral information retain in the fused results. The Corr values for the DRGT result is greater than from IHS, Brovey, and DWT. Also the IRGT results are greater even that from the DRGT fusion method. This means that the new methods are returned the better spectral information.

Table 2 lists the Corr values between the original PAN image and the new image bands. The higher Corr values between the panchromatic image and the fused image bands imply the improvement in spatial content when compared to the Corr values calculated for panchromatic and original multispectral image bands. The Corr values for DRGT and IRGT are greater than DWT, but their values less than the IHS and Brovey methods. Although this correlation is expected to

increase to a value closer to 1, it is not desirable because that will result in dominant spatial information in that corresponding band and loss of spectral information.

CONCLUSIONS

1. The Ridgelet and Improved Ridgelet fusion images have a very good spectral quality. The spatial quality of the fused images varies based on the data used for fusion.

2. In the Wavelet, Ridgelet, and Improved Ridgelet fusion methods, the spatial detail information is derived from the panchromatic image and added to the spectral information. But for other techniques, such as IHS and PCA, the spectral information is derived form the multispectral image and added to the panchromatic image.

3. By analyzing the subjective visual effect and objective statistic indicators evaluation, color distortion can be minimized by using Improved Ridgelet Transforms in fusion.

REFRENCES

Alpert B., Beylkin G., Coifman R., and Rokhlin V., *"Wavelet-like bases for the fast solution of second kind integral equations,"* SIAM J. Sci. Comput., VOL. 14, PP. 159–184, 1993.

Burrus C. S., Gopinath R. A., and Guo H., *"Introduction to Wavelets and Wavelet Transforms"* Prentice hall, 1998.

Daubechies I., *"Ten Lectures on Wavelets"* Philadelphia, PA: SIAM, 1992.

Dehghani M., *"Wavelet-based image fusion using "A trous" algorithm"* a M.Sc Thesis Submitted to Toosi University of Technology Vali_asr St, Tehran, Iran, P.C. 19697, 2003.

Eskicioglu A., Fisher P., *"Image quality measures and their performance"* IEEE Transactions on Communications, VOL. 43, NO.12, PP. 2959-2965, 1995.

Garzelli A., *"Possibilities and Limitations of the Use of Wavelets in Image Fusion"* a M.Sc Thesis Submitted to Department of Information Engineering DII, University of Siena, 2004.

Genderen V., *"Multisensor image fusion in remote sensing: concepts, methods and applications"* International Journal of Remote Sensing. VOL. 19, PP. 823-854, 1998.

Granai L. , *"Radon and Ridgelet transforms applied to motion compensated images"* Proceedings of the 2003 IEEE International Conference on Acoustics. Speech & Signal Processing ,2003.

Gungor O., Shan J., *"Evaluation of Satellite Image Fusion Using Wavelet Transform"* Geomatics Engineering, School of Civil Engineering, Purdue University, 550 Stadium Mall Drive, West Lafayette, IN 47907-2051, USA, 2003.

Panda G., Dash P. K., Pradhan A. K., and Meher S. K., *"Data Compression of Power Quality Events Using the Slantlet Transform"* IEEE Transactions On Power Delivery, VOL. 17, NO. 2, 2002.

Saleh Z. J., *"Video Image Compression based on Multiwavelets Transform"* a PHD Thesis submitted to university of Baghdad, 2004.

Selesnick I. W., *"The slantlet transform"* IEEE Transactions on Signal Processing, VOL. 47, PP. 1304–1313, 1999.

Vijayaraj V., *"A Quantitative Analysis of Pansharpened Images"* a M.Sc Thesis Submitted to the Faculty of Mississippi State University, 2004.